

Luminescent Neutral Platinum Complexes Bearing an Asymmetric N⁺N⁺N Ligand for High-Performance Solution-Processed OLEDs

Cristina Cebrián, Matteo Mauro, Dimitrios Kourkoulos, Pierluigi Mercandelli, Dirk Hertel, Klaus Meerholz, Cristian A. Strassert,* and Luisa De Cola*

In the past few decades, the search for highly emitting materials for electroluminescent devices has attracted a great deal of attention because of their potential applications in energy-saving organic light-emitting diodes (OLEDs) for full-color displays and solid-state lighting.^[1] Phosphorescent transition metal complexes are particularly appropriate for this purpose due to the strong spin-orbit coupling exerted by the heavy metal.^[2] This effect allows the harvest of both singlet and triplet electrogenerated excitons in devices containing such compounds, leading to a potentially achievable 100% internal quantum efficiency.^[2a,3] In this respect, a leading position is held by d⁶ octahedral iridium(III)^[4] and d⁸ square-planar platinum(II)^[5] complexes since they possess wide and tunable emission color range as well as high photoluminescence quantum yields (PLQYs).^[2a] However, the latter often have low solubility and strong tendency towards aggregation through platinum-platinum and π - π interactions,^[6] which hamper handling and purification, and in many cases have detrimental effects on photoluminescence properties.

Interestingly, while there are several reports on highly efficient iridium(III)-based light-emitting devices,^[7] the number of the platinum(II)-based counterparts is rather low, and only few showed comparable performances with the former ones.^[8] Amongst the possible ligands coordinated to the platinum ion, relevant role is played by the symmetric and asymmetric tridentate systems.^[9] In most cases the cyclometalated chelates have been used and to the best of our knowledge no complexes bearing an asymmetric dianionic N⁺N⁺N ligand

have been reported. Herein we present a new family of neutral platinum(II) complexes comprising this N⁺N⁺N-type chromophoric ligand that displays remarkable photophysical properties in solid state (Figure 1). The introduction of bulky and alkyl substituents into the structure enhanced solubility and processability of the final complexes, and prevented axial interactions between neighbor molecules.^[10] Even though these compounds showed poor photoluminescence quantum yield in fluid solution, their emission switched-on in solid state reaching the remarkable value of 0.61 in poly(methyl methacrylate) (PMMA) thin-film. By using these bulky asymmetric platinum complexes as triplet emitters in solution-processed polymer-based light-emitting diodes (PLEDs), power efficiency (PE) and external quantum efficiency (EQE) as high as 16.4 lm W⁻¹ and 5.6%, respectively, have been achieved. The attained results outperform the already reported PLED devices based on platinum(II) dopants and are approaching the more sophisticated, yet generally more efficient, vacuum-processed OLEDs.^[8a-c]

Since both 1,2,4-triazole and tetrazole rings bind to the platinum ion as anionic ligands by N-deprotonation,^[11] we have designed the asymmetric ligand 2-((3-adamantan-1-yl)-1H-1,2,4-triazol-5-yl)-6-(1H-tetrazol-5-yl)pyridine (**H₂trzpyttz**). It combines the dianionic nature, leading to neutral complexes upon Pt(II) coordination, with the possibility of easily substituting the tridentate (chromophoric) ligand for tuning the HOMO-LUMO gap. In order to obtain neutral platinum(II) complexes, ancillary ligands L such as triphenylphosphine and 4-amylypyridine were selected, yielding to the complexes **Pt(trzpyttz)phos** and **Pt(trzpyttz)py**, respectively. The synthesis is a one-pot reaction employing the asymmetric **H₂trzpyttz**, the desired L, PtCl₂(DMSO)₂ (DMSO = dimethylsulfoxide) as platinum(II) precursor, triethylamine as non-coordinating and non-nucleophilic base and acetonitrile as solvent.^[8d] The final compounds were easily purified by column chromatography and obtained

Prof. L. De Cola, Dr. C. A. Strassert, Dr. C. Cebrián,

Dr. M. Mauro

Physikalisches Institut and Center for

Nanotechnology (CeNTech)

Universität Münster

Heisenbergstrasse 11, 48149 Münster, Germany

Tel.: +49-251-53406957 or +49-251-53406906

Fax: +49-251-53406958

E-mail: ca.s@uni-muenster.de; decola@uni-muenster.de

Dr. Kourkoulos, Dr. D. Hertel, Prof. Dr. K. Meerholz

Department of Chemistry

Universität zu Köln

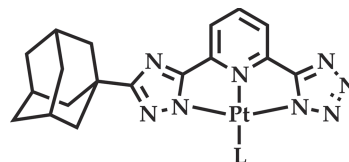
Luxemburger Strasse 116, 50939 Köln, Germany

Dr. P. Mercandelli

Department of Chemistry

Università degli Studi di Milano

Via Giacomo Venezian 21, 20133 Milan, Italy



Pt(trzpyttz)phos (L = PPh₃)

Pt(trzpyttz)py (L = 4-C₅H₁₁-py)

Figure 1. General molecular structure of complexes **Pt(trzpyttz)L**.

DOI: 10.1002/adma.201202123

Table 1. Photophysical properties of the complexes **Pt(trzpyttz)phos** and **Pt(trzpyttz)py** in solution in degassed THF, thin-film and 77 K 2-MeTHF rigid matrix.

Comp.	Medium (T) [K]	$\lambda_{\text{max,abs}} (\epsilon)$ [nm, $10^4 \text{ M}^{-1} \text{ cm}^{-1}$]	$\lambda_{\text{max,em}}^{\text{a,b}}$ [nm]	PLQY	τ_{obs}	k_r [10^4 s^{-1}]	k_{nr} [10^4 s^{-1}]
Pt(trzpyttz) phos	THF (298)	268 (8.1), 304 (1.5), 416 (0.07)	504, 532, 572(sh)	0.003	1 ns (75%), 94 ns (15%) ^{c)}	3.7	1228.7
	2-MeTHF (77)	-	483, 515, 552, 592(sh)		25.0 μs		
	PMMA 10 wt% (298)	-	504, 530	0.29	19.2 μs	1.5	3.7
	Neat film (298)	-	508(sh), 541	0.13	3.0 μs (10%), 11.1 μs (90%)	1.2	7.8
	Crystal (298)	-	483, 515, 552, 592(sh)	0.40	19.4 μs	2.1	3.1
Pt(trzpyttz) py	THF (298)	262 (2.6), 307 (1.7), 413 (0.07)	501, 528, 570(sh)	0.05	18 ns (15%), 751 ns (85%) ^{c)}	6.7	126.5
	2-MeTHF (77)	-	460, 493, 524, 575(sh)		16.0 μs		
	PMMA 10 wt% (298)	-	568	0.55	1.0 μs (73%), 9.9 μs (27%)	5.5	4.5
	Neat film (298)	-	573	0.60	0.8 μs (84%), 10.0 μs (16%)	6.0	4.0

^{a)}'sh' denotes a shoulder; ^{b)} λ_{exc} : 300 nm; ^{c)} λ_{exc} : 405 nm.

as microcrystalline yellow-green powders. They were fully characterized by using ^1H and ^{31}P NMR, high-resolution mass spectrometry and elemental analysis (see Schemes S1 and S2 of the Supporting Information).

Single crystals of the phosphine derivative **Pt(trzpyttz)phos**, suitable for X-ray diffractometric analysis, were obtained by slow diffusion of *n*-hexane into a concentrated dichloromethane solution at room temperature. In the complexes the platinum atom adopts a square-planar coordination geometry, distorted in order to comply with the constraints imposed by the tridentate ligand (Figure S1a). In particular, the N(trz)–Pt–N(py) and the N(ttz)–Pt–N(py) bond angles [78.50(11)° and 78.21(10)°, respectively] are narrower than expected for a square-planar complex. Steric hindrance between the adamantyl substituent on the triazole ring and the triphenylphosphine ancillary ligand results in a sensible deviation from planarity for the complex, as can be measured by the out-of-plane bending of the phosphorus atom of 8.92(17)°. The coordination mode of the triazole ring through its N(1) atom was confirmed.^[12] This result is in line with the known structures of platinum complexes with 1,2,4-triazolato ligands, which invariably adopts a κN^1 coordination mode.^[13] As far as the crystal packing is concerned, the complexes are oriented in a parallel head-to-tail staggered fashion, with alternating shorter and longer Pt...Pt distances (above 5 Å), ruling out the presence of any significant metal–metal interaction (Figure S1c). In addition, despite of the face-to-face arrangement of the tridentate ligands in nearby complexes (with an interplanar distance of ca. 3.2 Å), their interactions also appears to be negligible. Indeed, due to the presence of the bulky adamantyl and triphenylphosphine moieties, the ligands adopt a parallel-displaced arrangement and the shortest distances between the centroids of the heteroaromatic rings are larger than ca. 4 Å (Figure S1b).

For both complexes, geometrical optimization of their electronic ground state (S_0) was carried out by means of density functional theory (DFT) calculations at PBE0 level (see

Figure S2 and SI for computational details). In the case of **Pt(trzpyttz)phos**, the differences between calculated and experimental geometrical parameters were systematically below 1.5% (Table S1), confirming the suitability of the selected theoretical model. Moreover, for the most relevant frontier orbitals, partial molecular orbital diagram along with their isodensity surface plots and corresponding energies are shown in Figures S3 and S4 and Table S2, respectively. Despite the fact that the two complexes bear ancillary ligands with different electronic properties, they both show rather similar HOMO and LUMO, which are mainly localized on the tridentate ligand. In particular, the HOMO (–6.34 eV and –6.39 eV, for **Pt(trzpyttz)phos** and **Pt(trzpyttz)py**, respectively) appears to be the combination of π orbitals of the triazole (trz) and the d_{xz} orbitals of the platinum, with minor contribution of the π system of the pyridine (py) and tetrazole (tz). On the other hand, for both derivatives the LUMO lies at –2.28 eV and –2.36 eV, for **Pt(trzpyttz)phos** and **Pt(trzpyttz)py**, respectively (–3.51 eV and –3.48 eV as experimentally obtained by means of cyclic voltammetry, see Table S3 and Figure S5). Such virtual orbital displays a π^* character and is mostly centered on the pyridine moiety of the tridentate ligand, being the contribution of the metal and ancillary ligand orbitals negligible. Thus, the triazole and the pyridine of the tridentate ligand are expected to be strongly involved in the description of the low-lying excited states (see below).

The most meaningful photophysical data are listed in **Table 1** (extended version in Table S4), and the absorption and emission spectra displayed in **Figure 2**. In diluted tetrahydrofuran (THF) fluid solution, the complexes exhibit strong absorption bands ($\epsilon = 1.5\text{--}2.6 \times 10^4 \text{ M}^{-1} \text{ cm}^{-1}$) at high energy ($\lambda < 350 \text{ nm}$). These bands mainly correspond to convolution of singlet-manifold ligand-centered (^1LC) transitions involving the tridentate chromophoric ligand ($\pi\text{--}\pi^*$) with a minor contribution of metal-centered d orbitals, as evidenced by TD-DFT calculations (Figures 2a and S6a for **Pt(trzpyttz)phos**, Figures 2c and S6b for **Pt(trzpyttz)py** and Table S5). The low energy ($\lambda = 350\text{--}500 \text{ nm}$),

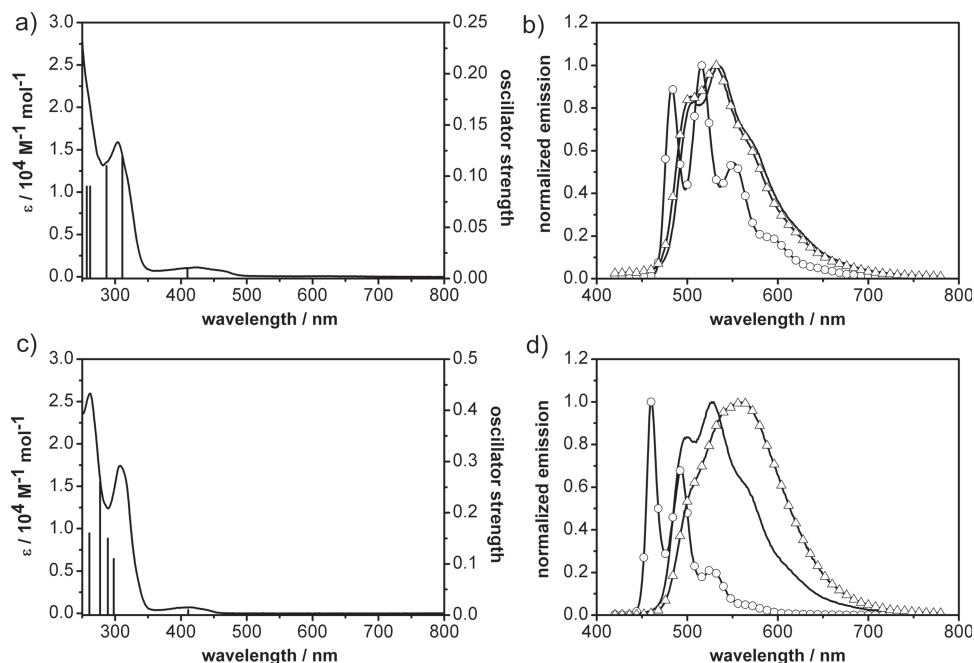


Figure 2. a) Absorption spectrum for complex **Pt(trzpyttz)phos** in fluid degassed THF solution. Calculated absorption peaks in vacuum are shown for comparison; b) emission spectra for complex **Pt(trzpyttz)phos** in fluid degassed THF (solid line), glassy 2-MeTHF (circles) and 10 wt% PMMA thin-film (triangles). $\lambda_{\text{exc}} = 300 \text{ nm}$; c) absorption spectrum for complex **Pt(trzpyttz)py** in fluid degassed THF solution. Calculated absorption peaks in vacuum are shown for comparison; d) emission spectra for complex **Pt(trzpyttz)py** in fluid degassed THF (solid line), glassy 2-MeTHF (circles) and 10 wt% PMMA thin-film (triangles). $\lambda_{\text{exc}} = 300 \text{ nm}$.

broader, featureless and less intense band ($\epsilon \approx 10^4 \text{ M}^{-1} \text{ cm}^{-1}$) represents the $S_0 \rightarrow S_1$ transition (HOMO \rightarrow LUMO), and mainly involves the platinum d orbitals (partially mixed with the π orbitals of the tridentate ligand) and π^* orbitals of the chelate. This transition is computed at 410 ($f = 0.01$) and 411 nm ($f = 0.01$) for **Pt(trzpyttz)phos** and **Pt(trzpyttz)py**, respectively, and can be ascribed to the spin-allowed singlet-manifold metal-ligand-to-ligand charge-transfer ($^1\text{MLLCT}$). Such findings are in nice agreement with similar already reported compounds.^[14] Upon excitation at 300 nm, in deaerated fluid THF solution at room temperature, both complexes showed structured emission in the green region of the visible spectrum, suggesting an emitting state with sizeable LC character (Figure 2b for **Pt(trzpyttz)phos** and Figure 2d for **Pt(trzpyttz)py**). The PLQYs are rather low in solution and the excited-state decays with multiexponential kinetics. Interestingly, the photophysics depend on the ancillary ligand since for **Pt(trzpyttz)phos** the emission quantum yield and excited state lifetimes are lower than for **Pt(trzpyttz)py**. This can be explained considering the distortion of the complex (see above) and therefore, a higher non-radiative constant (Table 1). Moreover, this intricate behavior could be further explained assuming thermally accessible dark states close to the emitting one (see below).^[15] The good solubility of these complexes allowed concentration studies in order to investigate the possible formation of aggregates, that were carried out on the flatter **Pt(trzpyttz)py** (Figure S7). Similarly to **Pt(trzpyttz)phos** in the crystalline state, **Pt(trzpyttz)py** did not seem to aggregate in solution within the 10^{-5} – 10^{-4} M concentration range, which strongly suggests that only one adamantyl group is enough for avoiding axial interactions in this kind of platinum complexes. Furthermore, for **Pt(trzpyttz)py** upon decreasing solvent polarity

from DMF to THF to toluene, a slight blue shift (163 cm^{-1}) was observed. Concomitantly, the emission displayed noticeable increase of the vibronic structure, followed by enhancement of PLQY and elongation of the excited state lifetime, that is monoexponential in the case of toluene solution (PLQY = 0.35, $\tau = 3.91 \mu\text{s}$) (Table S4, Figure S8). Going from fluid solution to 2-methyl-THF (2-MeTHF) glassy matrix at 77 K, the emission spectra showed hypsochromic shifts and even more pronounced vibronic progression attributable to intraligand modes (range 1230 – 1450 cm^{-1}),^[16] with monoexponential lifetimes of 25 and 16 μs , for complex **Pt(trzpyttz)phos** and **Pt(trzpyttz)py**, respectively, which is typical of phosphorescent platinum(II) complexes (Figures 2b and 2d). All these findings are indicative of the admixed metal-perturbed triplet-manifold ligand centered character of the radiative transition.^[14] Moreover, they support the presence of a thermally-accessible and strongly quenching state with intraligand charge-transfer (ILCT) nature, close in energy to the lowest-lying emitting one as depicted in Figure S9. For both complexes at their optimized T_1 state (see Table S6), the Lowest Singly Occupied Molecular Orbital (LSOMO) is located throughout the chromophoric ligand and the metal, whilst the Highest Singly Occupied Molecular Orbital (HSOMO) comprises only the triazole and the pyridine π systems, and it is slightly perturbed by the metal orbitals (Figure S10). Comparing **Pt(trzpyttz)phos** and **Pt(trzpyttz)py**, the calculated emission energies by means of ΔSCF technique (2.19 and 2.23 eV, respectively) nicely agree with the different emission energies observed at 77 K in 2-MeTHF (2.53 and 2.70 eV, respectively). Furthermore, complementary information are provided by analyzing plots of electron spin density and the difference in electron density between the excited state T_1 and the ground state S_0

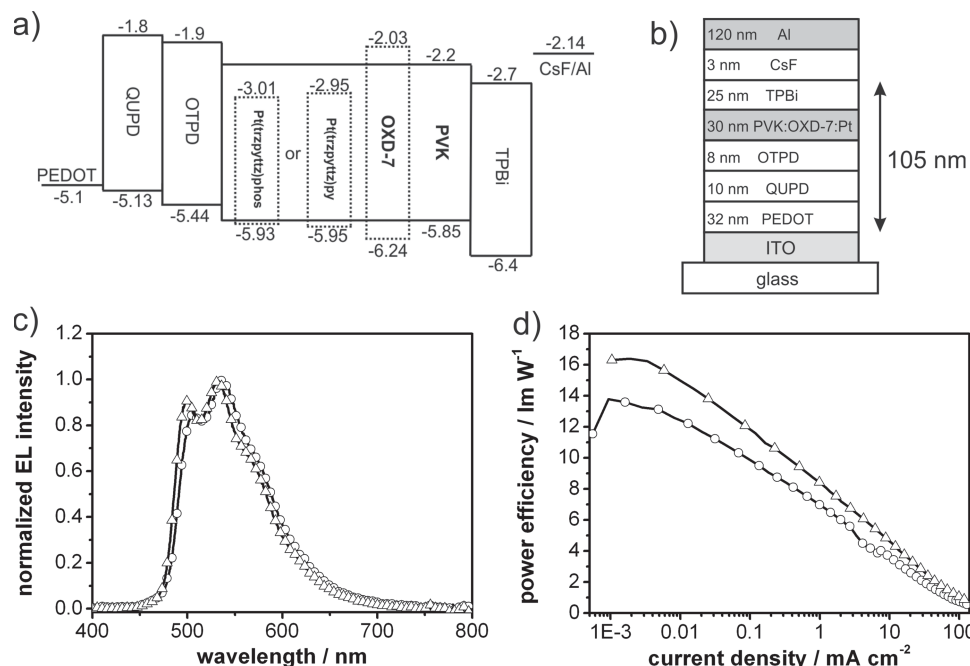


Figure 3. Electroluminescence (EL) characteristics of the device A and B, incorporating complex **Pt(trzpyttz)phos** and **Pt(trzpyttz)py**, respectively. The devices have the following architecture: ITO/PEDOT:PSS (32 nm)/QUPD (10 nm)/OTPD (8 nm)/PVK:OXD-7:platinum complex (30 nm)/TPBi (25 nm)/CsF (3 nm)/Al (120 nm). a) Schematic representation of the energy levels in the optimized devices; b) optimized device architecture; c) EL spectra of the device A (circles) and B (triangles) recorded at current density of 20 mA cm^{-2} ; d) power efficiency (PE) vs. current density plots for device A (circles) and device B (triangles).

computed at the T_1 optimized geometry (Figure S11) ($S_0 \leftarrow T_1$). Noteworthy, the triplet spin density is shared between triazole and pyridine rings, as well as the platinum atom, where also reorganization of the electron density takes place, confirming the admixed metal-perturbed ${}^3\text{LC}/{}^3\text{ILCT}$ character of the radiative deactivation process.

The luminescence efficiency of both derivatives was enhanced upon dispersion into PMMA rigid matrix. In particular, in the case of the bulkier **Pt(trzpyttz)phos**, no visible Pt...Pt interaction was observed going from solution to solid state, with PLQYs of 0.29 in 10 wt% PMMA thin-film and 0.40 in crystalline state, which is amongst the highest for a phosphorescent crystal at ambient temperature (see Figures 2b and S12a).^[17] Nonetheless, the behavior of the flatter **Pt(trzpyttz)py** respect to the former was remarkably different, displaying broad and featureless emission spectra for samples in thin films at any concentration level, with a concomitant bathochromic shift of ca. 46 nm (1518 cm^{-1}) (Figures 2d and S12b). The formation of a lower-lying excited-state upon establishment of π - π interactions in the solid state could account for such behavior. However, the rigid media contribute to the decrease of radiationless deactivation processes in comparison to fluid solution (Table 1), thus promoting the increase of the phosphorescence quantum yield, which reached values as high as 0.61 at 25 wt% doping concentration of **Pt(trzpyttz)py** in PMMA.

The appealing properties exhibited by **Pt(trzpyttz)phos** and **Pt(trzpyttz)py** such as good solubility in solvents like THF, low tendency towards aggregation and remarkably high PLQYs in solid state prompted us to investigate their application in electroluminescent devices. We constructed polymer-based devices

using different dopant/polymer ratios. The best devices were obtained when the platinum complexes were blended in a PVK/OXD-7 matrix, where PVK is poly(vinyl)carbazole and OXD-7 is 1,3-bis(*N,N*-t-butyl-phenyl)-1,3,4-oxadiazole. In such devices, the electron transporting material, namely OXD-7, was employed in order to improve the charge-transport properties of the matrix. The chemical structure of all the materials used for the device fabrication is given in Figure S13. The simplified architecture of the devices can be described as follows: ITO/PEDOT:PSS (32 nm)/QUPD (15 nm)/OTPD (13 nm)/PVK:OXD-7:platinum complex (40 nm)/CsF (3 nm)/Al (120 nm) (Figure S14). The HOMO and LUMO levels of the materials used in the devices are schematically depicted in Figure S15. The two cross-linkable hole transporting layers, namely *N,N'*-bis(4-[6-[(3-ethyloxetane-3-yl)methoxy]-hexyloxyphenyl]-*N,N'*-bis(4-methoxyphenyl)biphenyl-4,4'-diamine) (QUPD) and *N,N'*-bis(4-[6-[(3-ethyloxetane-3-yl)methoxy]-hexylphenyl]-*N,N'*-diphenyl-4,4'-diamine) (OTPD), were used to enhance the hole injection as well as for their electron blocking capabilities.^[18] The best electroluminescence (EL) performances were obtained when equimolar doping concentration of **Pt(trzpyttz)phos** and **Pt(trzpyttz)py**, 15.6 and 13.5 wt% respectively, were used into the host, resulting in devices with maximum PE of 3.9 and 4.7 lm W^{-1} , respectively.

To improve the charge balance and, hence, better positioning the recombination zone, an additional 1,3,5-tris(1-phenyl-1*H*-benzo[d]imidazol-2-yl)benzene (TPBi) layer was introduced acting as exciton/hole blocking and electron transport layer, while keeping similar the total thickness of the device. The energy level diagram is depicted in Figure 3a. The

simplified architecture of the devices can be described as follows: ITO/PEDOT:PSS (32 nm)/QUPD (10 nm)/OTPD (8 nm)/PVK:OXD-7:platinum complex (30 nm)/TPBi (25 nm)/CsF (3 nm)/Al (120 nm) (Figure 3b). As expected, the TPBi layer led to a significant improvement of the device performances. For Pt(trzpyttz)phos, maximum luminance efficiency (LE) of 13.4 cd A⁻¹ and PE of 13.8 lm W⁻¹ were obtained at the optimal 15.6 wt% doping concentration (device A), with maximum EQE of 4.9%. Moreover, it is noticeable that devices fabricated with Pt(trzpyttz)py as triplet emitter outperformed those with Pt(trzpyttz)phos when the best architecture device was used. In particular, the employment of 13.5 wt% Pt(trzpyttz)py allowed the achievement of high performances with peak LE of 15.5 cd A⁻¹, PE of 16.4 lm W⁻¹ and EQE as high as 5.6% (device B). Noteworthy, the here reported efficiencies, yet for simple solution-processed devices, approach the highest values ever reported for green emitting vacuum-processed OLEDs incorporating platinum(II)-based emitters.^[8a] The comparison of the EL spectra and PE vs. current density plots for devices A and B are shown in Figures 3c and 3d, respectively. The other current-voltage-luminance (*J-V-L*), EQE-*J* and EQE-*L* characteristics are depicted in Figure S16 and EL performances listed in Table S7. In such devices, the comparison of the EL spectra of Pt(trzpyttz)py with respect to Pt(trzpyttz)phos displays the expected slight hypsochromic shift of the emission (Figure 3c). Furthermore, both EL spectra are very similar to the corresponding photoluminescence (PL) spectra of the complexes in solution, as exemplary depicted for Pt(trzpyttz)py in Figure S17, supporting the idea that in such condition and for both compounds the same radiative transition is involved in both optical and electrically generated excited states. It is worth to notice that such findings rule out any significant Pt···Pt or π - π interactions between the dopant molecules in device condition, in spite of the relatively high dopant concentration, showing excellent color purity,^[19] with very weak voltage dependence of the emission spectra (Figure S18) and great stability (Figure S19).

In conclusion, we have shown that asymmetric dianionic tridentate ligands can be used to synthesize highly emitting neutral platinum complexes with improved solubility and suppressed aggregation tendency. The polymer-based devices, incorporating such compounds as triplet emitters, displayed noticeably good performances and high color purity, approaching those attained by the vacuum processed analogs.

Experimental Section

Details regarding the synthetic procedures, photophysical characterization, computational studies and device fabrication are described in the Supporting Information, and are available online from Wiley InterScience or from the authors. CCDC-879817 contains the crystallographic data for Pt(trzpyttz)phos·CH₂Cl₂. These data can be obtained free of charge from the Cambridge Crystallographic Data Centre.

Acknowledgements

The authors would like to thank the German Federal Ministry for Education and Research (BMBF) for funding with the project no. 13N10529 (So-light). CC acknowledges the University of Castilla-La

Mancha, DAAD and BMBF for financial support. MM gratefully thanks the Alexander von Humboldt Foundation for financial support. Alessandro Aliprandi is gratefully acknowledged for the electrochemical measurements.

Received: May 27, 2012

Revised: July 23, 2012

Published online:

- [1] W. Brütting, J. Frischeisen, B. J. Scholz, T. D. Schmidt, *Europhysics News* **2011**, 42, 20.
- [2] a) H. Yersin, in *Highly Efficient OLEDs with Phosphorescent Materials*, Wiley-VCH, Weinheim, Germany **2008**; b) M. E. Thompson, P. E. Djurovich, S. Barlow, S. Marder, Organometallic Complexes for Optoelectronic Applications, in *Comprehensive Organometallic Chemistry III*, (Eds: R. H. Crabtree, D. M. P. Mingos), Elsevier, Oxford, UK **2006**; c) Y. Chi, P.-T. Chou, *Chem. Soc. Rev.* **2010**, 39, 638.
- [3] M. A. Baldo, D. F. O'Brien, A. Shoustikov, S. Sibley, M. E. Thompson, S. R. Forrest, *Nature* **1998**, 395, 151.
- [4] L. Flamigni, A. Barbieri, C. Sabatini, B. Ventura, F. Barigelletti, *Top. Curr. Chem.* **2007**, 281, 143.
- [5] a) J. Kalinowski, V. Fattori, M. Cocchi, J. A. G. Williams, *Coord. Chem. Rev.* **2011**, 255, 2401; b) K. M.-C. Wong, V. W.-W. Yam, *Coord. Chem. Rev.* **2007**, 251, 2477.
- [6] a) W. B. Connick, D. Geiger, R. Eisenberg, *Inorg. Chem.* **1999**, 38, 3264; b) D. K. C. Tears, D. R. McMillin, *Coord. Chem. Rev.* **2001**, 211, 195; c) Y. Zhang, H. Zhang, X. Mu, S.-W. Lai, B. Xu, W. Tian, Y. Wang, C.-M. Che, *Chem. Comm.* **2010**, 46, 7727; d) A. Díez, J. Forniés, C. Larraz, E. Lalinde, J. A. López, A. Martín, M. T. Moreno, V. Sicilia, *Inorg. Chem.* **2010**, 49, 3239; e) A. Kobayashi, H. Hara, T. Yonemura, H.-C. Chang, M. Kato, *Dalton Trans.* **2012**, 41, 1878; f) A. Barbieri, G. Accorsi, N. Armaroli, *Chem. Comm.* **2008**, 2185.
- [7] For the best devices see: a) R. Wang, D. Liu, H. Ren, T. Zhang, X. Wang, J. Li, *J. Mater. Chem.* **2011**, 21, 15494; b) N. Choupra, J. Lee, Y. Zheng, S.-H. Eom, J. Xue, F. So, *Appl. Phys. Lett.* **2008**, 93, 143307.
- [8] a) A. Y.-Y. Tam, D. P.-K. Tsang, M.-Y. Chan, N. Zhu, V. W.-W. Yam, *Chem. Comm.* **2011**, 47, 3383; b) U. S. Bhansali, E. Polikarpov, J. S. Swensen, W. H. Chen, H. Jia, D. J. Gaspar, B. E. Gnade, A. B. Padmaperuma, M. A. Omary, *Appl. Phys. Lett.* **2009**, 95, 233304; c) M. Cocchi, J. Kalinowski, L. Murphy, J. A. G. Williams, V. Fattori, *Org. Electron.* **2010**, 11, 388; d) C. A. Strassert, C.-H. Chien, M. D. Galvez-Lopez, D. Kourkoulos, D. Hertel, K. Meerholz, L. De Cola, *Angew. Chem. Int. Ed.* **2010**, 50, 946.
- [9] a) G. S.-M. Tong, C.-M. Che, *Coord. Chem. Rev.* **2002**, 229, 113; b) F. N. Castellano, I. E. Pomestchenko, E. Shikhova, F. Hua, M. L. Muro, N. Rajapakse, *Coord. Chem. Rev.* **2006**, 250, 1819; c) Z. Wang, E. Turner, V. Mahoney, S. Madakuni, T. Groy, J. Li, *Inorg. Chem.* **2010**, 49, 11276; d) E. Rossi, A. Colombo, C. Dragonetti, D. Roberto, F. Demartin, M. Cocchi, P. Brulatti, V. Fattorie, J. A. G. Williams, *Chem. Comm.* **2012**, 48, 3182; e) G. S.-M. Tong, C.-M. Che, *Chem. Eur. J.* **2009**, 15, 7225; f) K.-W. Wang, J.-L. Chen, Y.-M. Cheng, M.-W. Chung, C.-C. Hsieh, G.-H. Lee, P.-T. Chou, K. Chen, Y. Chi, *Inorg. Chem.* **2010**, 49, 1372; g) S. C. F. Kui, F.-F. Hung, S.-L. Lai, M.-Y. Yuen, C.-C. Kwok, K.-H. Low, S. S.-Y. Chui, C.-M. Che, *Chem. Eur. J.* **2011**, 18, 96; h) J. Li, Z. Wang, E. Turner, PCT Int. Pat. Appl. WO **2009** 111299 A2.
- [10] X.-H. Zhao, G.-H. Xie, Z.-D. Liu, W.-J. Li, M.-D. Yi, L.-H. Xie, C.-P. Hu, R. Zhu, Q. Zhao, Y. Zhao, J.-F. Zhao, Y. Qiana, W. Huang, *Chem. Comm.* **2012**, 48, 3854.
- [11] a) P. Coppo, E. A. Plummer, L. De Cola, *Chem. Commun.* **2004**, 1774; b) E. Orselli, G. S. Kottas, A. E. Konradsson, P. Coppo, R. Fröhlich,

- L. De Cola, A. van Dijken, M. Büchel, H. Börner, *Inorg. Chem.* **2007**, 46, 11082.
- [12] M. Duati, S. Tasca, F. C. Lynch, H. Bohlen, J. G. Vos, S. Stagni, M. D. Ward, *Inorg. Chem.* **2003**, 42, 8377.
- [13] a) A. I. Matesanz, P. Souza, *J. Inorg. Biochem.* **2007**, 101, 245; b) H.-Y. Hsieh, C.-H. Lin, G.-M. Tu, Y. Chi, G.-H. Lee, *Inorg. Chim. Acta* **2009**, 362, 4734.
- [14] M. Mydlak, M. Mauro, F. Polo, M. Felicetti, J. Leonhardt, G. Diener, L. De Cola, C. A. Strassert, *Chem. Mater.* **2011**, 23, 3659.
- [15] Y.-S. Yeh, Y.-M. Cheng, P.-T. Chou, G.-H. Lee, C.-H. Yang, Y. Chi, C.-F. Shu, C.-H. Wang, *ChemPhysChem.* **2006**, 7, 2294.
- [16] A. F. Rausch, L. Murphy, J. A. G. Williams, H. Yersin, *Inorg. Chem.* **2012**, 51, 312.
- [17] a) E. Q. Procopio, M. Mauro, M. Panigati, D. Donghi, P. Mercandelli, A. Sironi, G. D'Alfonso, L. De Cola, *J. Am. Chem. Soc.* **2010**, 132, 14397; b) N. Komiya, M. Okada, K. Fukumoto, D. Jomori, T. Naota, *J. Am. Chem. Soc.* **2011**, 133, 6493.
- [18] P. Zacharias, M. C. Gather, M. Rojahn, O. Nuyken, K. Meerholz, *Angew. Chem. Int. Ed.* **2007**, 46, 4388.
- [19] V. Adamovich, J. Brooks, A. Tamayo, A. M. Alexander, P. I. Djurovich, B. W. D'Andrade, C. Adachi, S. R. Forrest, M. E. Thompson, *New J. Chem.* **2002**, 26, 1171.